

Structural basis for basal activity and auto-activation of ABA signaling SnRK2 kinases

Ley-Moy Ng ^{1,2*}, Fen-Fen Soon ^{1,2*}, X. Edward Zhou ^{1*}, Graham M. West ³, Amanda Kovach ¹, Kelly M. Suino-Powell ¹, Michael J. Chalmers ³, Jun Li ^{1, 2}, Eu-Leong Yong², Jian-Kang Zhu^{4,5}, Patrick R. Griffin ³, Karsten Melcher ^{1§}, and H. Eric Xu ^{1,6§}

Supporting Information

This supplement contains:

SI Materials and Methods

Figs. S1 to S9

Table S1

SI Materials and Methods

Protein preparation. Wild type and mutant SnRK2s were expressed in *E. coli* BL21 (DE3) as H6Sumo fusion proteins and purified following the same general method as described previously for the purification of PYL1 (1). Briefly, proteins were first purified by Ni-chromatography, followed by proteolytic cleavage of the H6Sumo tag and dialysis. The cleaved H6Sumo tag was removed by re-binding to a Nickel HP column, and further purified by gel filtration chromatography (HiLoad 26/60 Superdex 200) in 25 mM Tris, pH8.0, 200 mM ammonium acetate, 1 mM dithiothreitol and 1 mM EDTA. HAB1 was purified as described (1). We generated a total of 10 sets of SnRK2.3 (D41A/K41A, E46A, D57A/K58A, D60A/E61A, R191A/Q192A/E193A, K197A, E222A/E223A, R225A, K280A, E298A) and 11 sets of SnRK2.6 (D40A/K41A, E45A, E56A/K57A, D59A/E60A, K190A/K191A/E192A, K196A, E221A/E222A, K224A, K264A, K279A, D296A/E297A) surface entropy mutants. Mutated residues were predicted to be solvent-exposed and within flexible loops based on the position of the homologous amino acids in the Snf1 structure. All mutant proteins were catalytically active and interacted with HAB1, but only SnRK2.3 D57A/K58A and SnRK2.6 D59A/E60A yielded diffraction quality crystals.

Hydrogen/Deuterium Exchange and Mass Spectrometry. Solution phase HDX experiments were performed with a LEAP Technologies Twin HTS PAL liquid handling robot interfaced with an Orbitrap mass spectrometer (Exactive, ThermoFisher Scientific) (2). SnRK2 solutions were prepared at 15 μ M by diluting stocks detailed in the Proteins Preparation section above into a buffer consisting of 25 mM Tris HCl, 200 mM ammonium acetate, 1 mM EDTA, 1 mM DTT at pH 8.0. These 15 μ M solutions were diluted 1:4 into the same buffer dissolved in D₂O buffer (or H₂O buffer for “0 second” samples) and incubated for predetermined times (10, 30, 60, 300, 900 and 3600 seconds) at 4°C before quenching. Quenching was performed by combining 20 μ L of incubating kinase solution with 30 μ L of 3 M Urea in 1.0% TFA at 1°C. Digestion was performed in line with chromatography using an in-house packed pepsin column (3) at 50 μ l/min and peptides were captured and desalted on a 2 mm i.d. C8 trap (Thermo Fisher Scientific, San Jose, CA). Peptides were then separated across a 10x1 mm (5 μ m) Hypersil Gold C8 column (Thermo Fisher Scientific, San Jose, CA) with a linear gradient of 12-40% acetonitrile in 0.3% formic acid over five minutes. Peptide ion signals were confirmed if they had a MASCOT score of 20 or greater and had no ambiguous hits using a decoy (reverse) sequence in a separate experiment using a 60 minute gradient. The intensity weighted average m/z value (centroid) of each peptide's isotopic envelope was calculated with the in-house developed software HD Desktop (4) and corrected for back-exchange.

To determine the phosphorylation status of SnRK2s, peptides corresponding to phosphorylated and unphosphorylated ion signals were sequenced in separate MS/MS experiments. Kinases in these MS/MS experiments were incubated in the presence and absence of ATP (1 hour ATP incubation). All samples, for both MS/MS experiments and MS experiments, contained 10 μ M kinase, 10 mM Mg²⁺, and 0.2 mM ATP. HAB1 was at 10 μ M when present. Ratios of phosphorylated to unphosphorylated peptide were calculated from area under the curve measurements of monoisotopic ion signals.

Kinase Assays. SnRK2 kinases were either pre-incubated with HAB1 in kinase buffer (25 mM Tris, pH 7.4, 12 mM MgCl₂, 2 mM DTT) for 30 minutes at room temperature or were directly incubated with 0.2 mM unlabelled ATP, 2.5 μCi [³²P]-γATP, and 2 μM GST-ABF2(73-120) for 30 min (or the indicated amount of time in Fig. 1A) at room temperature in a total volume of 15 μl. Reactions were terminated by addition of SDS sample buffer and subjected to Tricine SDS-PAGE. Gels were stained with Coomassie and subjected to autoradiography using a FLA-5000 phosphor imager (Fuji).

AlphaScreen assays. Interactions between SnRK2s and HAB1 were assessed by luminescence-proximity AlphaScreen technology as described previously (1). Reactions contained 100 nM recombinant H6GST-SnRK2.6 proteins bound to nickel-acceptor beads and 100 nM recombinant biotin-HAB1 bound to streptavidin donor beads.

Mutagenesis. Site-directed mutagenesis was carried out using the QuikChange method (Agilent). Mutations and all plasmid constructs were confirmed by sequencing.

Thermoshift assay. Reactions were set up in final volumes of 10 μl in 96-well plates with 10x SYPRO Orange (Invitrogen), using the StepOnePlus™ Real-Time PCR System (Applied Biosystems) melt curve program with a ramp rate of 1 °C and temperature range of 15 °C to 85 °C.

Supplemental References

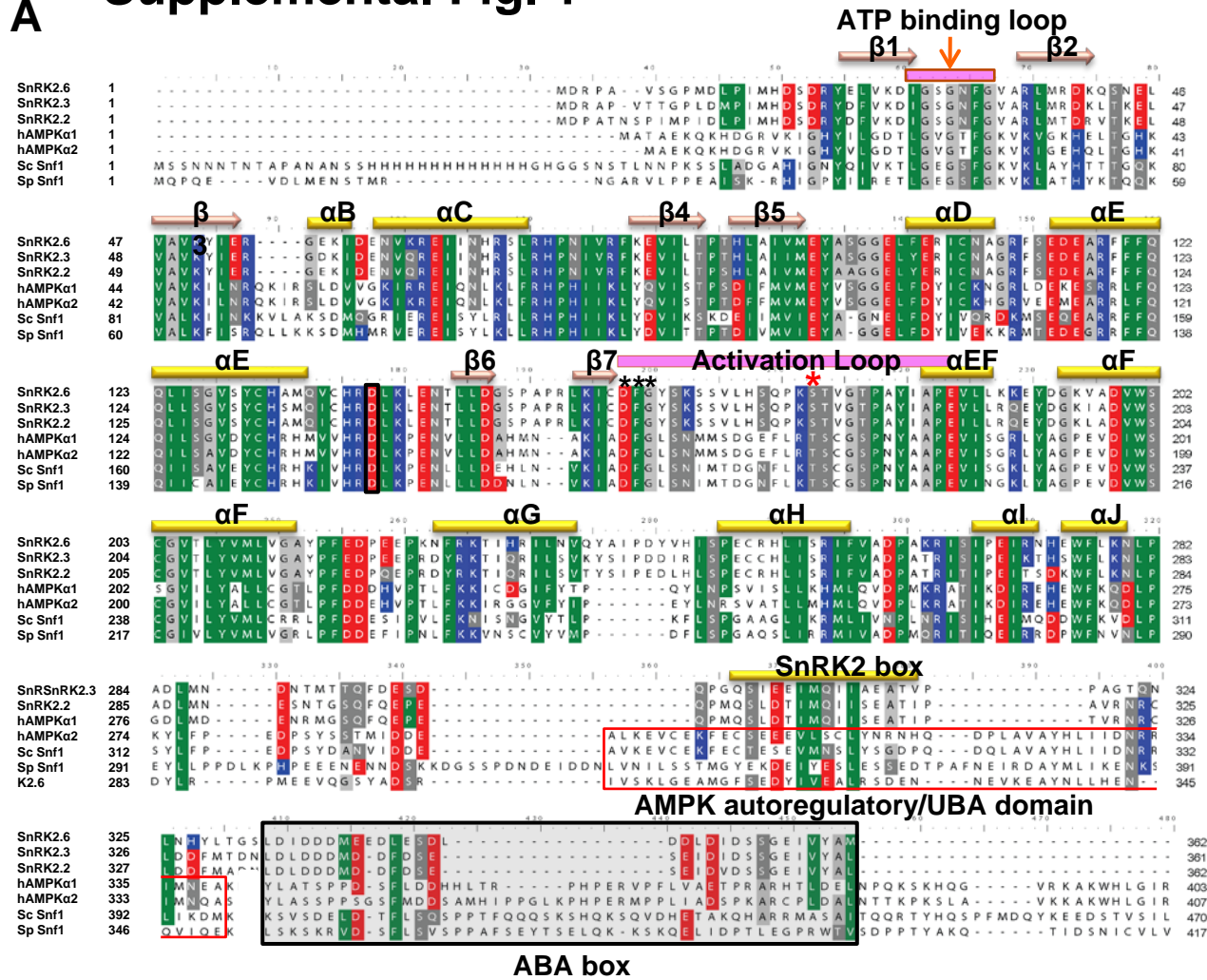
1. Melcher, K., Ng, L. M., Zhou, X. E., Soon, F. F., Xu, Y., *et al.* (2009) A gate-latch-lock mechanism for hormone signalling by abscisic acid receptors. *Nature* 462: 602-608.
2. Chalmers, M. J., Busby, S. A., Pascal, B. D., He, Y., Hendrickson, C. L., *et al.* (2006) Probing protein ligand interactions by automated hydrogen/deuterium exchange mass spectrometry. *Anal. Chem.* 78: 1005-1014.
3. Busby, S. A., Chalmers, M. J., & Griffin, P. R. (2007) Improving digestion efficiency under H/D exchange conditions with activated pepsinogen coupled columns. *Int. J. Mass Spect.* 259: 130-139.
4. Pascal, B. D., Chalmers, M. J., Busby, S. A., & Griffin, P. R. (2009) HD desktop: an integrated platform for the analysis and visualization of H/D exchange data. *J. Am. Soc. Mass Spectrom.* 20: 601-610.

Supplemental Table 1:

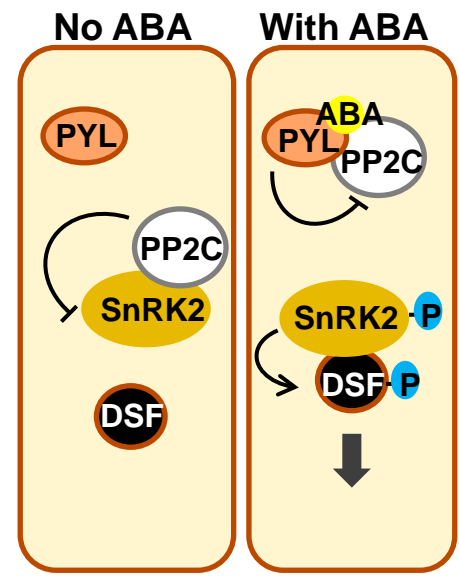
Statistics of data sets and structure refinement

	SnRK2.3	SnRK2.6
PDB code	3UC3	3UC4
Data collection		
APS beam line	21-ID-F	21-ID-D
Space group	P3 ₁ 21	C222 ₁
Resolution, Å	30-1.90	30-2.30
Cell parameters, Å, °	a=75.41, b=75.41, c=116.434; $\alpha=\beta=90$, $\gamma=120$	a=76.11, b=171.54, c=116.24; $\alpha=\beta=\gamma=90$
Total/Unique reflections	209703 /30806	216364/34851
Completeness, %	100.0 (100.0)	100.0 (100.0)
I/ σ	20.77 (3.3)	19.7 (2.9)
Redundancy	6.8 (6.8)	6.2 (6.3)
R _{sym}	0.079 (0.594)	0.086 (0.653)
Structure Determination		
Resolution, Å	30-1.90	30-2.30
No. reflections	28568	31695
Molecules per A.U.	1	2
No. residues	271	574
No. solvent molecules	143	115
No. of non-H atoms	2332	4726
R _{cryst}	21.2%	22.0%
R _{free}	22.9%	24.6%
rmsd bonds, Å	0.008	0.012
rmsd angles, °	1.065	1.171
Average B factor, Å ²	25.69	40.11

A Supplemental Fig. 1



B



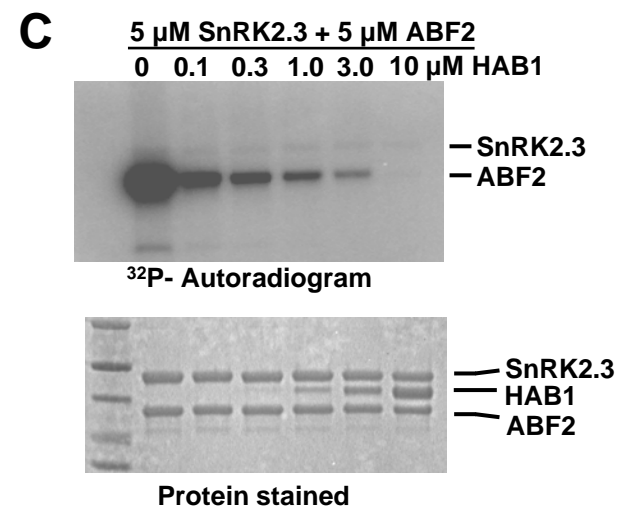
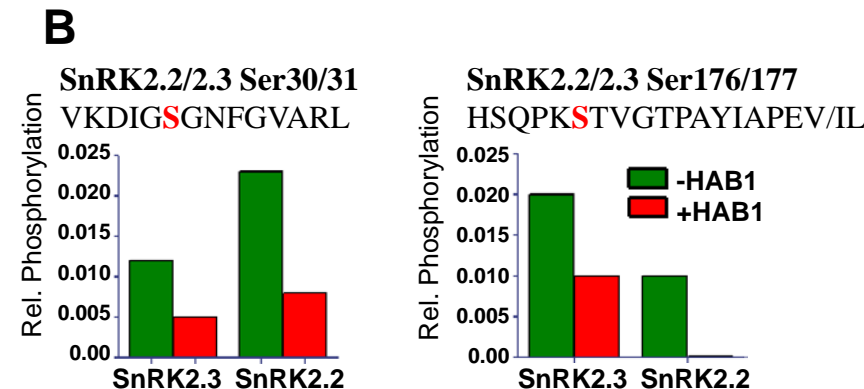
*S175

Supplemental Figure 1: SnRK2 sequence and model of SnRK2/ABA signaling. (A) Structure-based sequence alignment of the three SnRK2s with the α 1 and α 2 subunits of human AMPK and *S. cerevisiae* and *S. pombe* Snf1. Secondary structure elements and the ATP binding loop, activation loop, SnRK2 box, AMPK autoregulatory/Uba domain (red box), and ABA box (shaded rectangle) are indicated. The conserved DFG motif of the Mg²⁺-binding loop is indicated by asterisks. The alignment was performed using BioEdit, with the program ClustalW and the similarity matrix BLOSUM62 using default parameters. (B) Cartoon presentation (modified from 11) of the core ABA signaling pathway. In the absence of ABA, the SnRK2 kinases are inhibited by PP2Cs. In the presence of ABA, the PYL ABA receptors form a complex with ABA and PP2Cs that inhibits PP2C catalytic activity, allowing SnRK2 autoactivation and phosphorylation of downstream factors (DSFs).

Supplemental Fig. 2

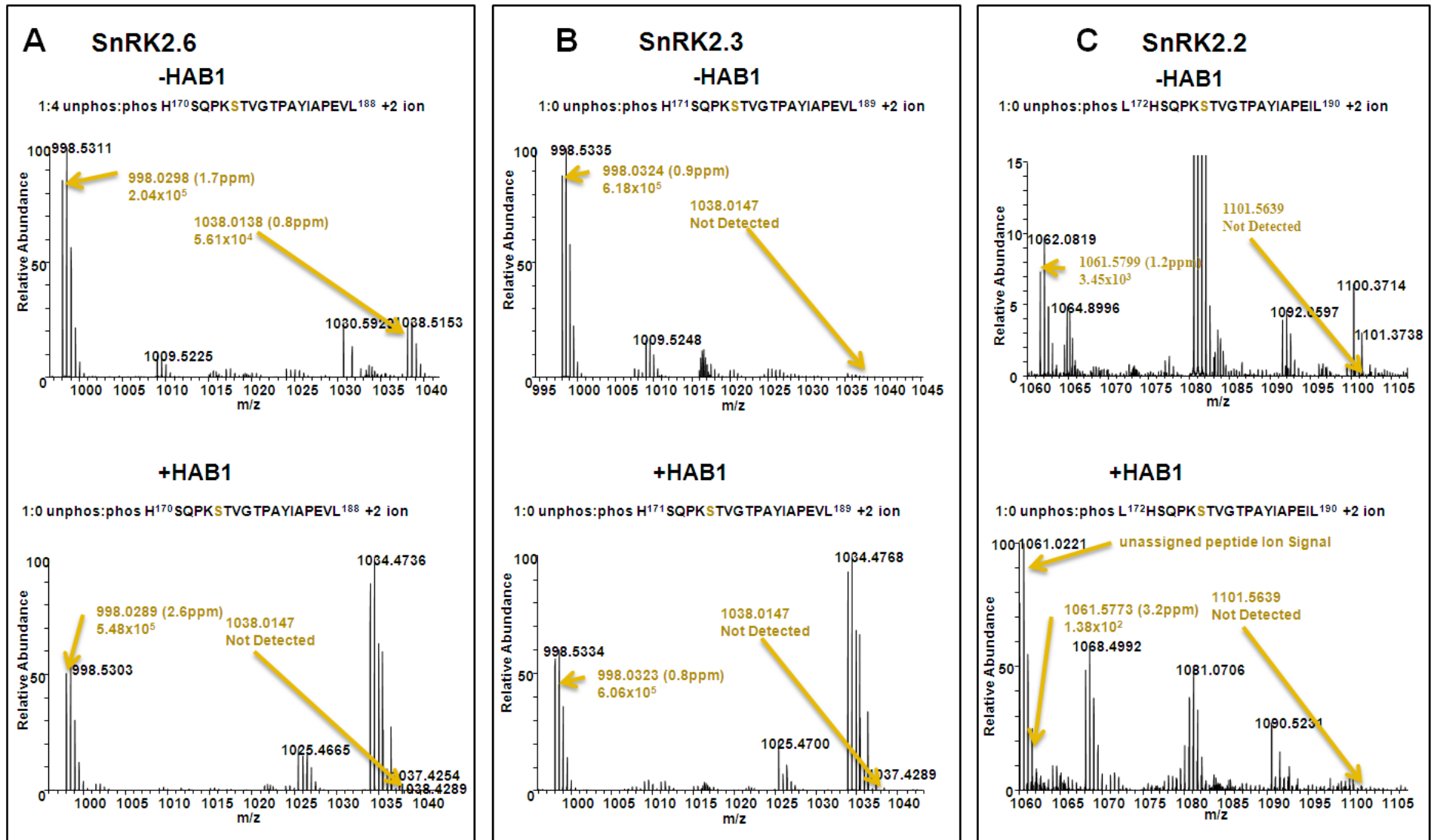
A

SnRK2.6		SnRK2.6 + HAB		SnRK2.3		SnRK2.2	
sequence	z	sequence	z	sequence	z	sequence	z
S7: GSMDRPAVSGPM	1					S7: GSMDPATNSPIMPIDL	2
S7: GSMDRPAVSGPM	2						
S7: GSMDRPAVSGPMDL	2						
S7: GSMDRPAVSGPMDL PIMHDSDRYELVKDI GSGNFGVARL	3						
S29: LVKDIGSGNFGVARL	2					S31: FVKDIGSGNFGVARL	2
S29: VKDIGSGNFGVARL	2	S29: VKDIGSGNFGVAR	2	S30: VKDIGSGNFGVARL	2	S31: VKDIGSGNFGVARL	2
S175/T176: HSQPKSTVGTPAYIA PEVL	2						
S175/T176: HSQPKSTVGTPAYIA PEVLLKKEYDGKVAD VWSCGVTL	4						
				S203: LRQEYDGKIADVWSCG	2		



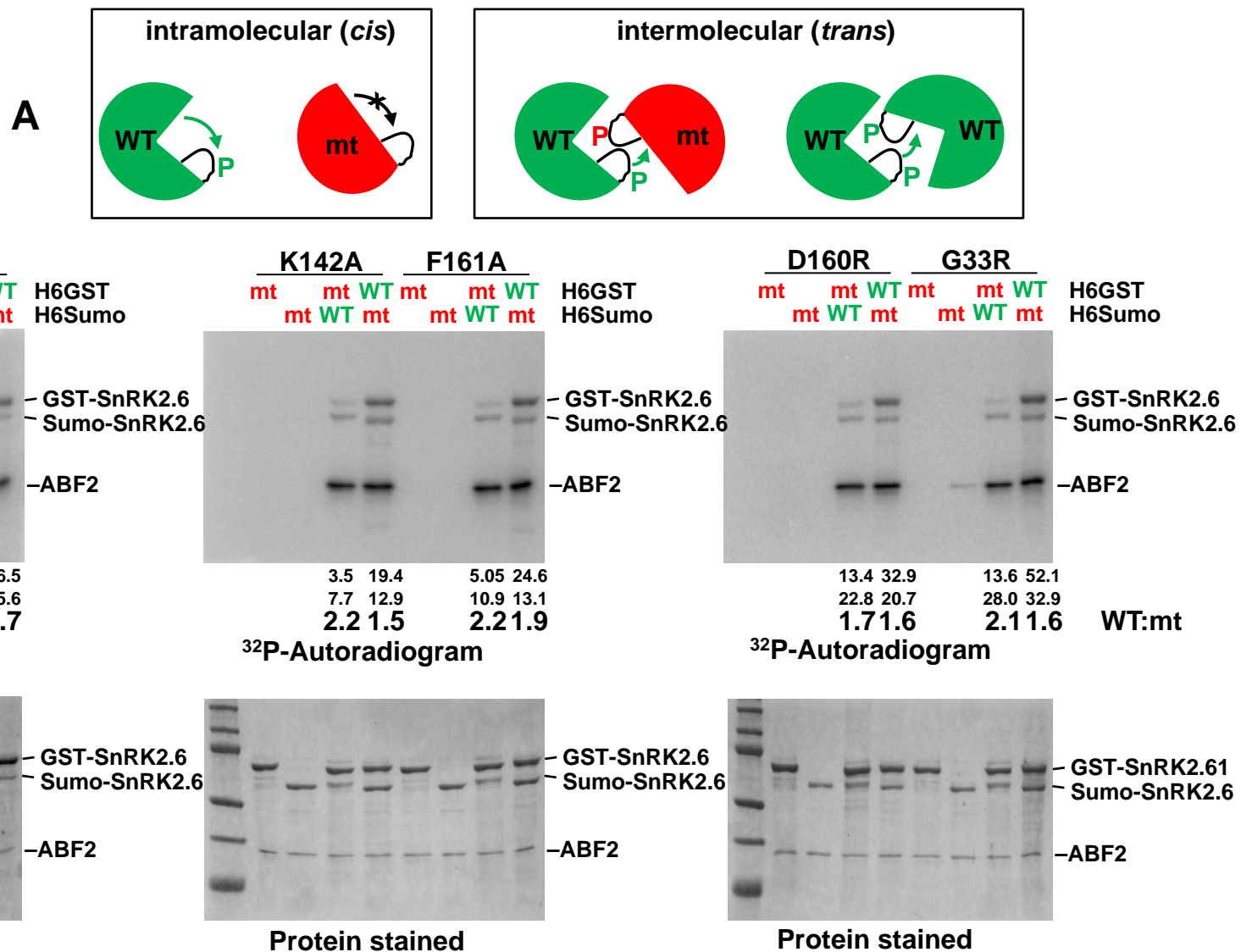
Supplemental Figure 2: Activation loop phosphorylation of recombinant SnRK2s in the presence and absence of HAB1. (A) Determination of phosphorylation sites in SnRK2s by mass spectrometry. Sequences of peptides with phosphorylated residues identified by mass spectrometry. Peptide coverage SnRK2.2: 93%, 2.3: 96%, 2.6: 68%, 2.6+HAB1: 79%. (B) Comparison of the ratio of phosphorylated and unphosphorylated peptides from N-terminus (/30/31) and activation loop (/176/177) of SnRK2 kinases in the presence of ATP and the presence and absence of HAB1 (see Methods). For comparison, the ratio for SnRK2.6 Ser 29 is 3 (without HAB1) and 1.5 (with HAB1) and for activation loop Ser 175 is 3 (without HAB1) and 0.03 (with HAB1) (22). (C) Inhibition of SnRK2.3 activity by HAB1. Increasing amounts of HAB1 were added to a kinase reaction with 5 μ M SnRK2.3 and 1 μ M ABF2. At high HAB1 concentrations, SnRK2.3 activity is completely inhibited. Similar inhibition has been seen for SnRK2.6 (22).

Supplemental Fig. 3



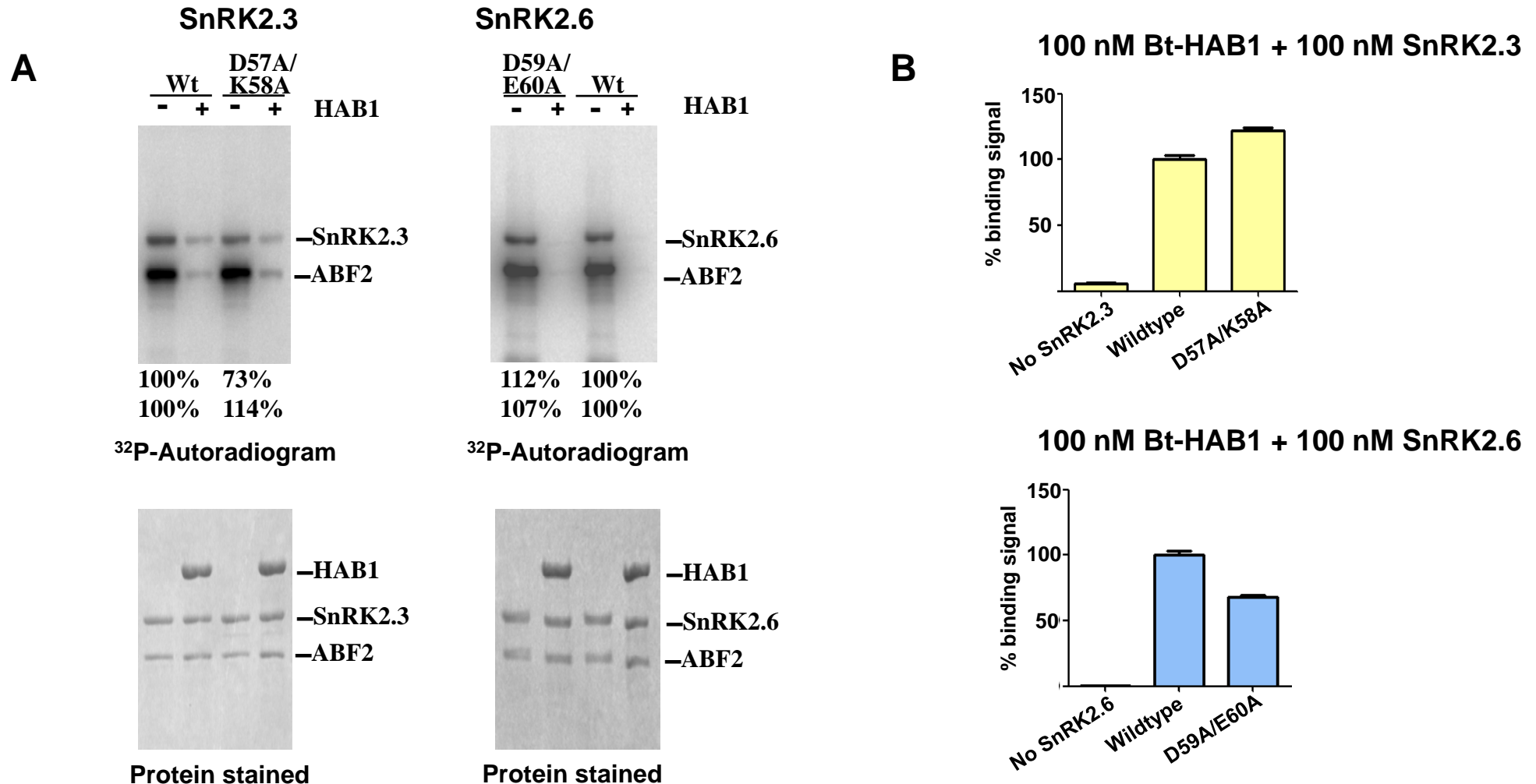
Supplemental Figure 3: Activation loop phosphorylation of recombinant SnRK2s in the presence and absence of HAB1. (A-C) Relative S175 (SnRK2.6) (A), S176 (SnRK2.3) (B), and S177 (SnRK2.2) (C) phosphorylation levels were measured by mass spectrometry based on relative ion signals intensities. The mass spectra shown have been selected from control samples in HDX experiment that did not contain D₂O. No ATP was present in these samples. The ion signal intensities are listed below the masses when detected. Arrows mark the monoisotopic ion signals of unphosphorylated and phosphorylated activation loop peptides within 5 ppm of the theoretical m/z. Top: Mass spectra of SnRK2 peptides in the absence of HAB1. Bottom: Mass spectra of SnRK2 peptides in the presence of HAB1.

Supplemental Fig. 4



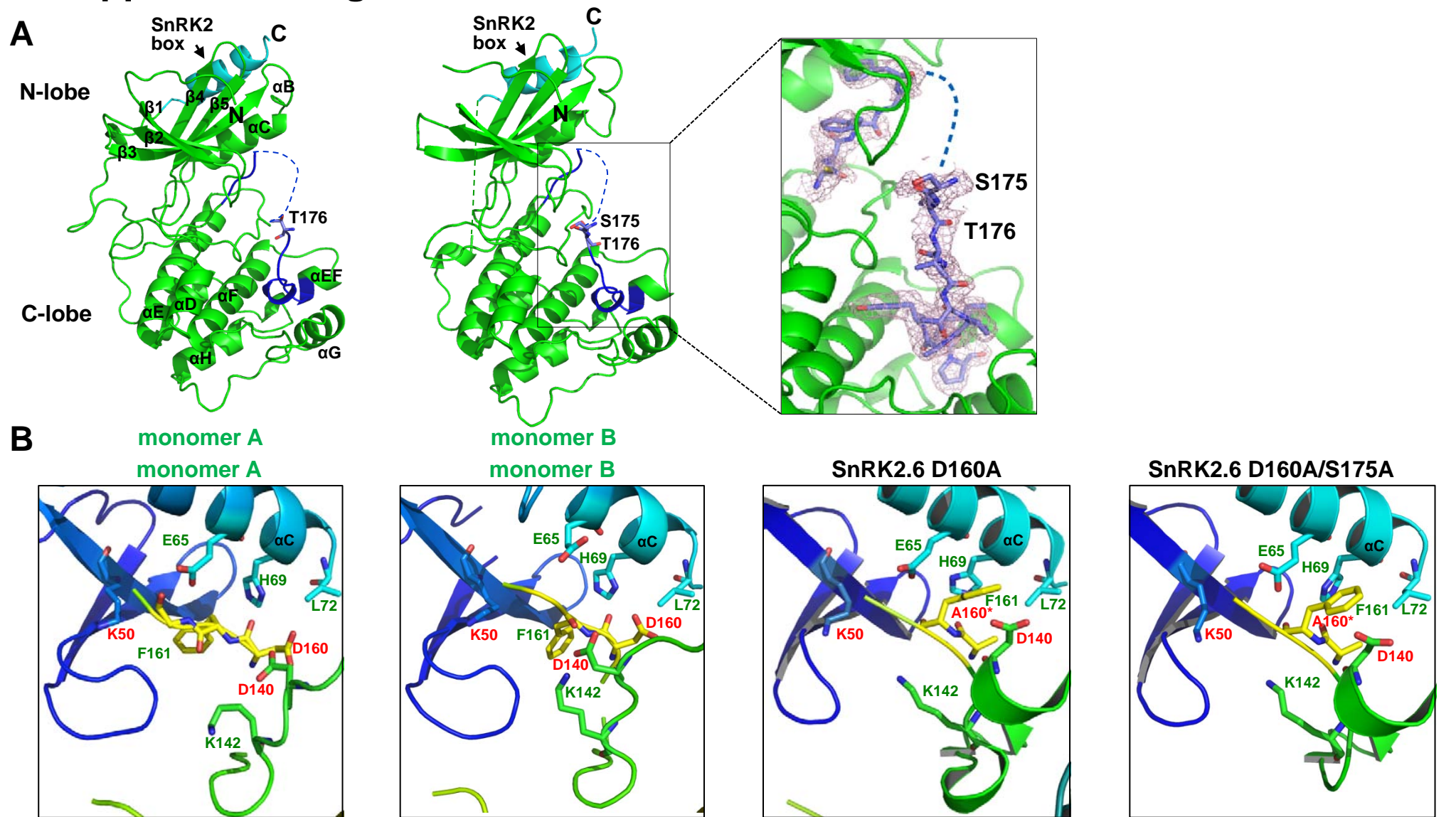
Supplemental Figure 4: SnRK2.6 *trans* and *cis* autophosphorylation. (A) Cartoon outlines of the experimental design and expected results to distinguish *trans* and *cis* phosphorylation of SnRK2.6 kinase. *Cis* autophosphorylation would cause [³²P]-phosphate incorporation into wildtype SnRK2.6 only, while *trans* autophosphorylation would cause equal incorporation into wildtype and mutant SnRK2.6. (B) Kinase reactions employing wildtype and mutant SnRK2.6 fused to either the larger H6GST tag (GST-SnRK2.6) or the smaller H6Sumo tag (Sumo-SnRK2.6). Note that with the exception of the naturally occurring SnRK2.6 G33R mutant none of the SnRK2.6 mutants displayed kinase activity under these reaction conditions. Numbers below autoradiogram: densitometry of H6GST-SnRK2.6 and H6Sumo-SnRK2.6, normalized to the amount of proteins loaded, and the ratios of normalized wildtype (WT) to mutant (mt) phosphorylation bands.

Supplemental Fig. 5



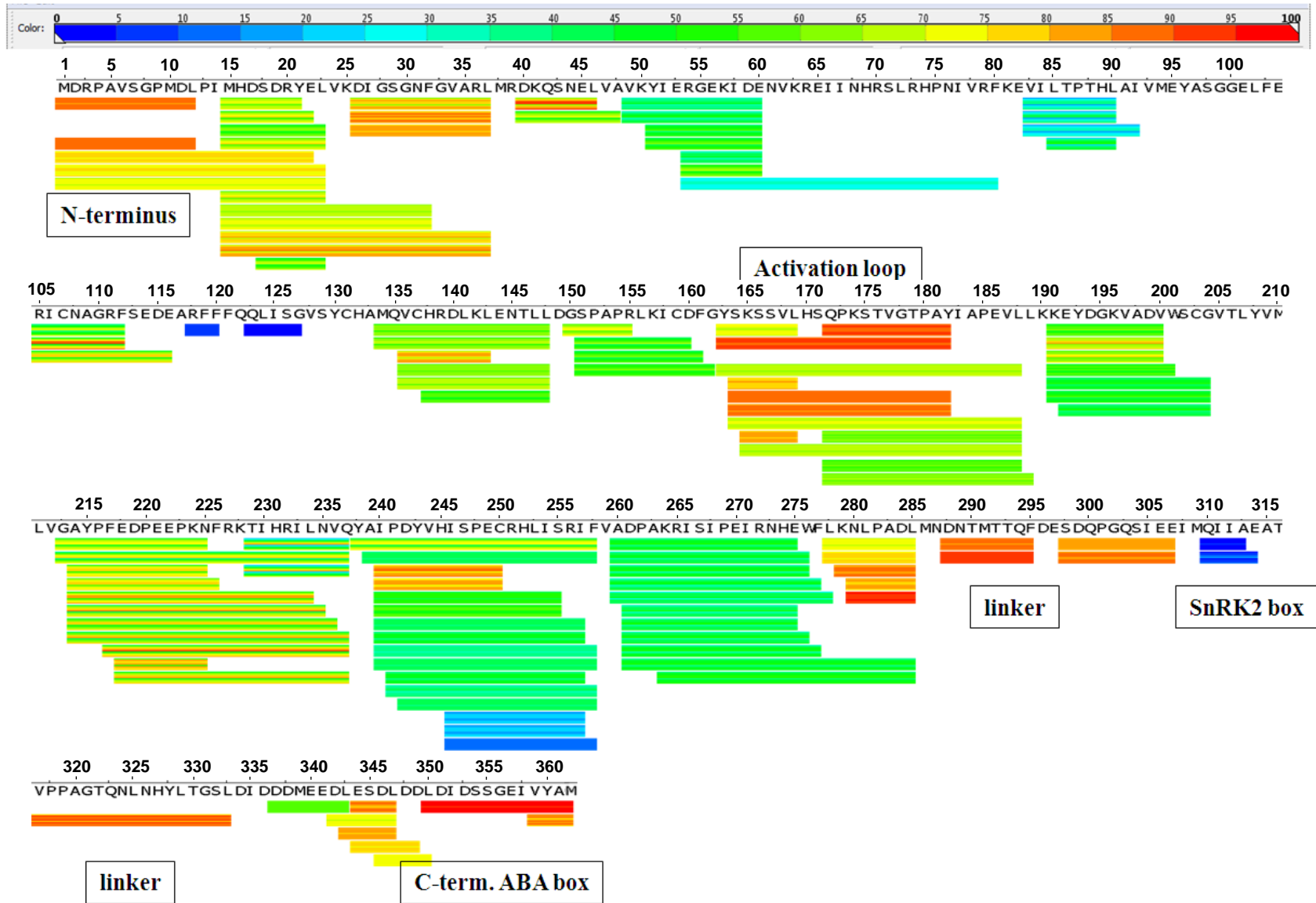
Supplemental Figure 5: SnRK2 surface entropy reduction mutant proteins are active. (A) Kinase assays of SnRK2.3 and 2.6 wildtype and mutant proteins in the absence and presence of HAB1. Shown are the results for the two mutants that have yielded crystal structures: E56A/K57A (apo SnRK2.3) and D59A/E60A (apo SnRK2.6). Numbers below autoradiogram: densitometry of autophosphorylation (top) and ABF2 phosphorylation bands relative to wildtype. (B) AlphaScreen luminescence proximity interaction assays between biotinylated MBP-HAB1 (Bt -HAB1) and wildtype and mutant H6GST-SnRK2.3 and -2.6 proteins. Error bars indicate SD (n = 3).

Supplemental Fig. 6



Supplemental Figure 6: SnRK2.6 structure comparison. (A) Structures of the two SnRK2.6 monomers found in the SnRK2.6 asymmetric unit. Ser175 and Thr176 from the activation loop are shown in stick presentation, parts of SnRK2.6 not resolved in the structures are indicated as dashed lines. The activation loop area of monomer B is shown as detail with $2F_o - F_c$ composite omit map of the activation loop contoured at 1σ . (B) Side-by-side views of the reaction centers of the two SnRK2.6 monomers from the asymmetric unit and of the two catalytically inactive mutants (D160A mutation marked by an asterisk) described in (42). The asymmetric units of the two mutant proteins contained one more monomer, each, with all monomers being very similar to each other (43).

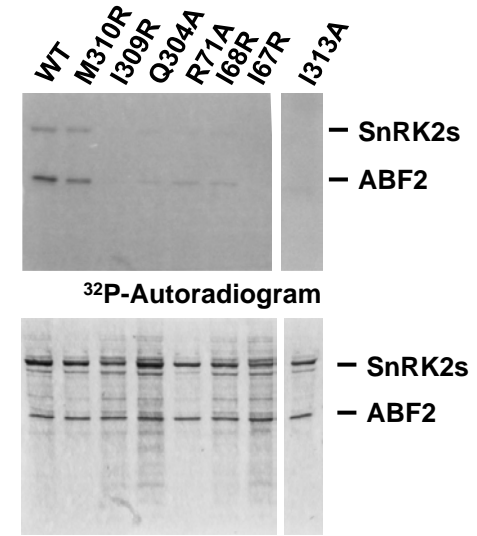
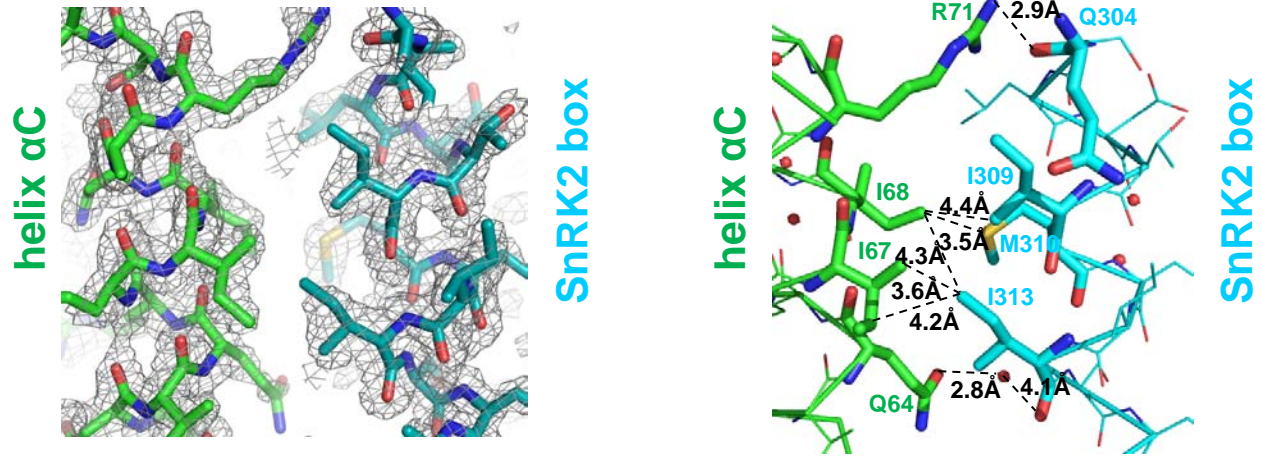
Supplemental Fig. 7



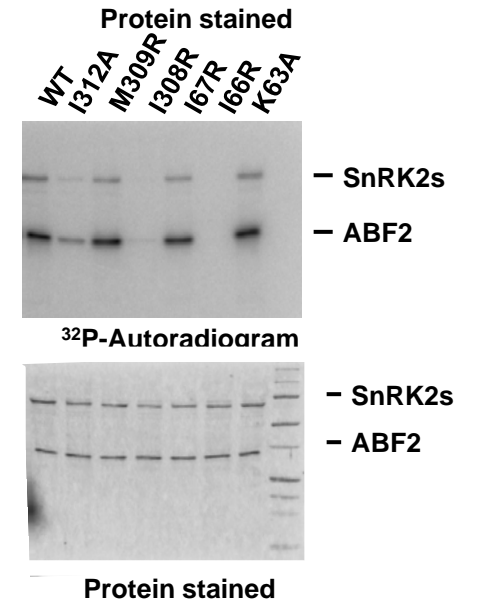
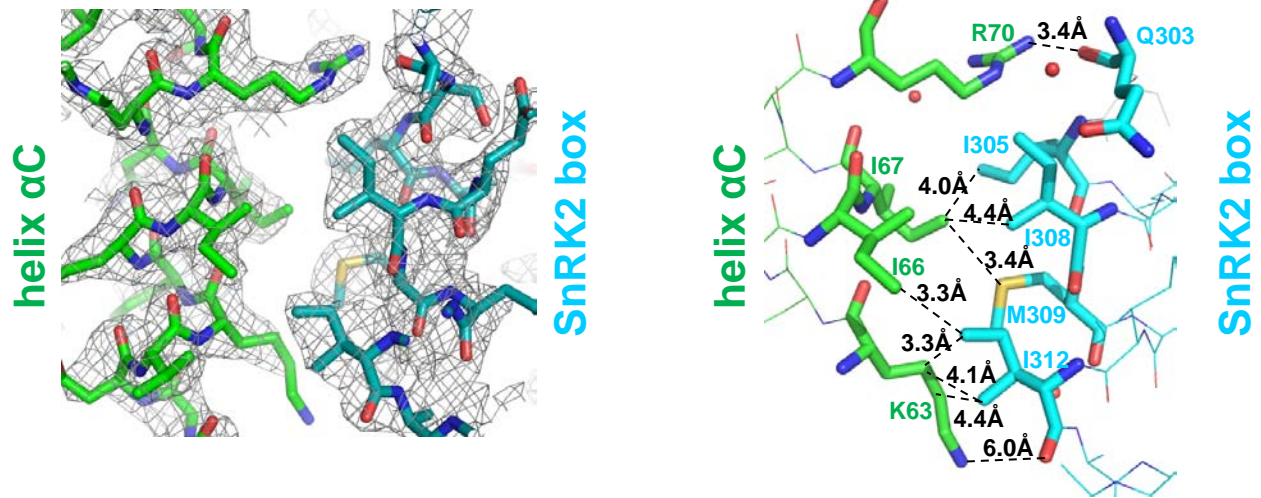
Supplemental Figure 7: HDX protection map of apo SnRK2.6. The bars below the sequence represent the peptide fragments resolved by mass spectrometry and the bar colors represent the relative deuterium/hydrogen exchange (color code on top). Amino acid positions of the SnRK2.6 protein are indicated above the sequence.

Supplemental Fig. 8

A: SnRK2.3

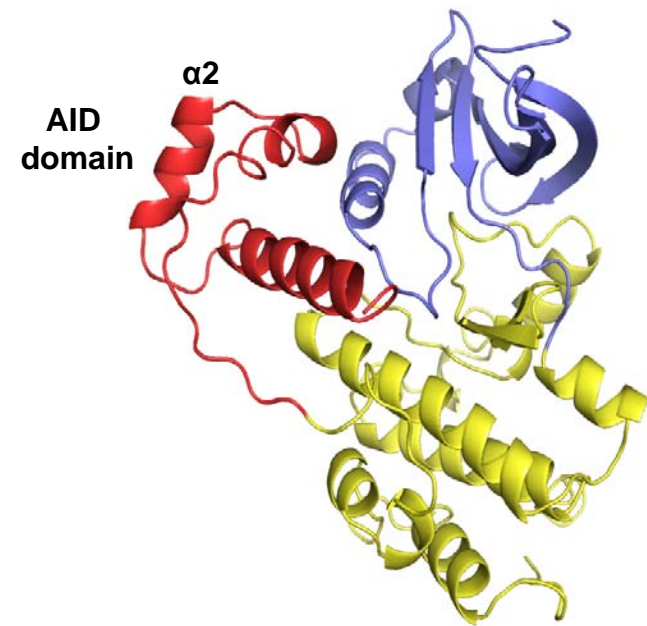
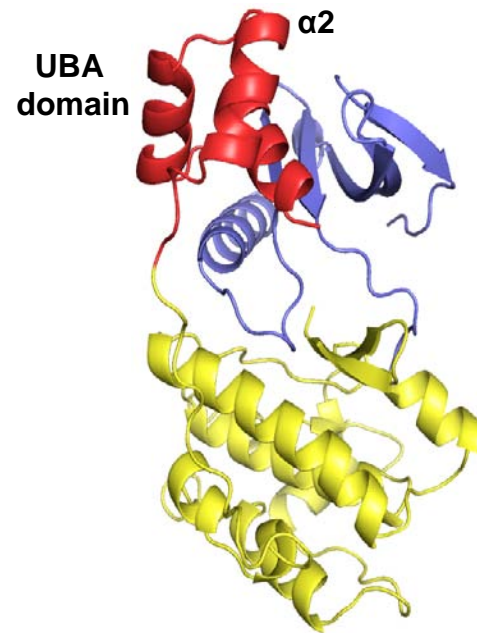
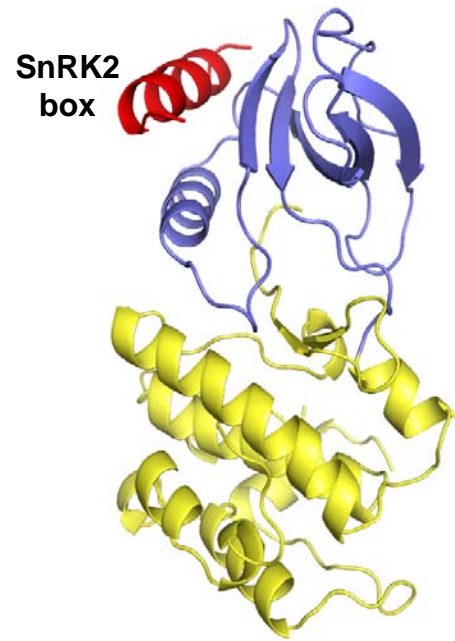


B: SnRK2.6



Supplemental Figure 8: The SnRK2 box– α C interaction is required for SnRK2 activity. (A) SnRK2.3, (B), SnRK2.6 (monomer A). *Left:* $2F_o-F_c$ composite omit maps contoured at 1.0σ of the interaction surfaces between α C (green) and SnRK2 box (cyan) helices. *Middle:* SnRK2 box– α C interaction maps. The helices are shown as line presentations with key residues shown as stick models. Water molecules are indicated as red balls and bonds as dashes with distances indicated in Å. *Right:* Kinase assays using wildtype and mutant SnRK2.3 and SnRK2.6.

Supplemental Fig. 9



Supplemental Figure 9: Comparison of the SnRK2 box, UBA domain, and AID domain of AMPK-related kinases. Ribbon diagrams with the large and small lobes of the kinase domains shown in yellow and blue and the accessory domains in red.